PHYSICAL REVIEW E **77**, 065201(R) (2008)

Chaotic soliton walk in periodically modulated media

Dmitry Turaev,[1] Mindaugas Radziunas,[2] and Andrei G. Vladimirov[2,3]
[1]*Ben Gurion University, 84105 Be'er Sheva, Israel*
[2]*Weierstrass Institute for Applied Analysis and Stochastics, Mohrenstrasse 39, D-10117 Berlin, Germany*
[3]*Physics Faculty, St. Petersburg State University, Ulianovskaya 3, 198504 St. Petersburg, Russia*
(Received 12 October 2007; revised manuscript received 24 March 2008; published 9 June 2008)

We show that a weak transverse spatial modulation in (2+1) nonlinear Schrödinger-type equation can result in nontrivial dynamics of a radially symmetric soliton. We provide examples of chaotic soliton motion in periodic media both for conservative and dissipative cases. We show that complex dynamics can persist even for soliton sizes greater than the modulation period.

DOI: 10.1103/PhysRevE.77.065201 PACS number(s): 05.45.−a, 42.65.Sf, 42.65.Tg

Equations of nonlinear Schrödinger type play a central role in understanding various phenomena in plasma physics, hydrodynamics, Bose-Einstein condensation, and nonlinear optics. For example, they describe pulse propagation in nonlinear fibers and self-focusing of paraxial beams of light in a homogeneous Kerr medium [1]. In the case of purely cubic nonlinearity, (2+1)-dimensional nonlinear Schrödinger (NLS) equation possesses a localized solution, "the Townes mode" [2]. However, this solution is always unstable: small perturbations lead to a collapse, an unbounded growth of the field amplitude within a finite time. A suppression of the collapse can be achieved by various means [3,4]: thus, replacing the cubic nonlinearity with a saturable one is an efficient way of the collapse arrest that leads to a stable self-collimated propagation of a light beam. In a spatially homogeneous medium the paraxial beam propagates with a constant velocity along a straight line. However, because of recent developments in fabrication of microstructured waveguiding materials [5], there is a growing interest to the study of nonlinear beam propagation in various inhomogeneous settings [1,4,6–9].

In this Rapid Communication we study mobility properties of stable solitons of conservative and dissipative NLS-type equations in the situation where the refractive index of the medium is subjected to a weak periodic modulations in two transverse directions. Using multiscale method, we derive equations which describe the soliton as a Newtonian particle in the external potential created by the refractive index profile. Surprisingly, the soliton motion equations remain Hamiltonian even in the case of dissipative nonlinearity; as we show, the effect is a consequence of the Galilean symmetry of the NLS-type equations.

The soliton-particle analogy is known to be useful for the analysis of soliton interaction [10–14]. However, in the studies of soliton dynamics in spatially modulated media the effective particle approach was mostly applied in nearly integrable one-dimensional settings [15–17]. Our method is free of these restrictions; furthermore, the results remain valid independently of the ratio of the soliton transverse size to the modulation period, even when the soliton is quite wide.

We show that similar to a particle in a two-dimensional potential, the soliton in the medium with a transversely modulated refractive index can move both in a regular and chaotic manner, and the choice between these two types of motion is foremost determined by the geometry of the refractive index profile. When the refractive index forms a rectangular lattice, the effective potential is integrable, and the soliton transverse motion is very close to the integrable one for long time intervals. In this case there are two typical dynamical regimes: the first corresponds to low-energy quasiperiodic oscillations around local maximum of the refractive index (minimum of the effective potential), the second corresponds to quasiperiodic oscillations superimposed on a constant velocity drift. In the case of hexagonal lattice the situation is drastically different. Here, with the increase of the soliton kinetic energy the oscillations near a local maximum of refractive index become chaotic and transform into a random walk—an unbounded transverse motion of the soliton wandering chaotically between different cells of the refractive index profile. Thus, our results show that even in simple periodic media a soliton can exhibit very complicated motion patterns.

While the results apply to any nonlinear Galilean-invariant (2+1) equation, we focus here on the simplest example written in the dimensionless form

$$\partial_t A = i(\partial_{xx}A + \partial_{yy}A) + Af(|A|^2) + i\varepsilon^2 g(\mathbf{r})A, \qquad (1)$$

where $\mathbf{r}=(x,y)$ is the radius vector in the transverse plane and $A(\mathbf{r},t)$ is the normalized complex field amplitude. Note that when f is purely imaginary, Eq. (1) is Hamiltonian, with the energy functional $H=\frac{1}{2}\int[|\partial_x A|^2+|\partial_y A|^2+\Phi(|A|^2)-\varepsilon^2 g(x,y)|A|^2]dxdy$, where $\Phi' \equiv if$. The conservation of energy H means that the purely imaginary f corresponds to light propagation in a transparent medium. To ensure the stability of the soliton, we use the saturable Kerr-type nonlinearity [3]

$$f(|A|^2) = -i(1+|A|^2)^{-1}, \qquad (2)$$

typical, e.g., for photorefractive media [1].

An important feature of Eq. (1) is that at $\varepsilon=0$ it is invariant with respect to the Galilean transformation to a moving coordinate frame,

$$A(\mathbf{r},t) \to A(\mathbf{r}-\mathbf{v}t,t)\exp(i\mathbf{r}\cdot\mathbf{v}/2 - i|\mathbf{v}|^2 t/4). \qquad (3)$$

It follows that for $\varepsilon=0$ any stationary solution of Eq. (1) coexists with a family of uniformly moving solutions parametrized by the velocity vector $\mathbf{v}$.

The term $i\varepsilon^2 g$ in Eq. (1) with small ε and real $g(\mathbf{r})$ describes the spatial variation of the refractive index profile. If

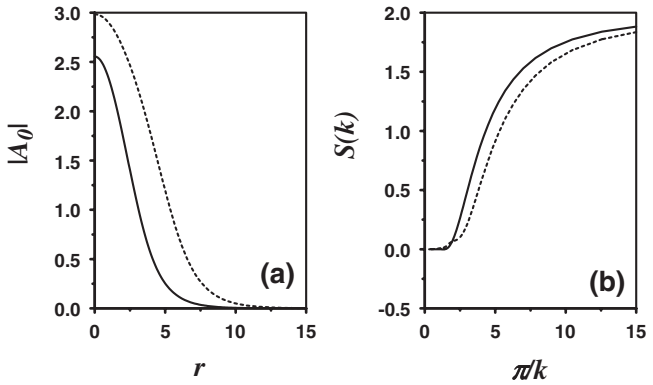

FIG. 1. Soliton amplitude profiles (a) and response functions (b). Solid lines correspond to conservative nonlinearity (2). Dotted lines correspond to dissipative nonlinearity (4) with $G=2.11$, $Q=2.0$, and $s=10$.

$g(\mathbf{r}) \neq \text{const}$, the translational and, hence, Galilean symmetries are broken at nonzero ε, which results in a nontrivial motion of the soliton in the (x,y) plane.

The propagation of paraxial light beams in a dissipative media can be described by the same equation (1), where the function f in the right-hand side is no longer purely imaginary. In our simulations we take f real,

$$f(|A|^2) = -1 + G(1+|A|^2/s)^{-1} - Q(1+|A|^2)^{-1}, \qquad (4)$$

where G and Q are linear gain and, respectively, absorption coefficients, and $s>1$ is the ratio of the saturation intensities of the gain and absorber media. Equation (1) with nonlinearity (4) was used to describe pattern formation in broad area lasers with saturable absorbers [18].

In the dissipative case, the Hamiltonian structure of the equation is lost, while the Galilean symmetry is preserved at $\varepsilon=0$. We show that this results in a great similarity of the soliton motion in the conservative and dissipative cases, in spite of the difference between the physical mechanisms of the soliton formation.

Let Eq. (1) at $\varepsilon=0$ have a radially symmetric stationary soliton $A(\mathbf{r},t)=A_0(r)e^{i\omega_0 t}$, where $A_0 \to 0$ exponentially fast as $r \to \infty$ (we denote $r=|\mathbf{r}|$). Since the equation at $\varepsilon=0$ is symmetric with respect to spatial translations, the vector-function $\mathbf{U}=\nabla A=\mathbf{r}A_0'(r)/r$ satisfies $L\mathbf{U}=0$, where the operator $L: X \mapsto [i(\Delta-\omega_0)+f(E_0)+E_0 f'(E_0)]X+A_0^2 f'(E_0)X^*$ yields the linearization of the right-hand side of Eq. (1) at the soliton solution. Here the star denotes complex conjugation, and $E_0=|A_0|^2$. Galilean symmetry of Eq. (1) implies the existence of the vector-function $\mathbf{Z}$ such that $L\mathbf{Z}=\mathbf{U}$. By differentiating formula (3) with respect to $\mathbf{v}$, we find that $\mathbf{Z}=-i\mathbf{r}A_0(r)/2$.

Let us define the inner product of functions X and Y as follows: $\langle X,Y\rangle=\int(XY+X^*Y^*)dxdy$. According to this definition, the adjoint to L operator $L^\dagger$ reads as $L^\dagger: X \mapsto [i(\Delta-\omega_0)+f(E_0)+E_0 f'(E_0)]X+[A_0^2 f'(E_0)]^*X^*$. Like L, the operator $L^\dagger$ has a nontrivial odd solution to $L^\dagger\mathbf{U}^\dagger=0$. Due to the rotational symmetry, $\mathbf{U}^\dagger=\mathbf{r}U^\dagger(r)/r$, where $U^\dagger(r)$ is a scalar function. An easy computation gives $\langle Z_x, U_y^\dagger\rangle=\langle Z_y, U_x^\dagger\rangle=0$ and $\langle Z_x, U_x^\dagger\rangle=\langle Z_y, U_y^\dagger\rangle=\int\Psi(r)dxdy$, where $\Psi(r)=\int_r^{+\infty}\mathrm{Im}[U^\dagger(\rho)A_0(\rho)]d\rho$, and $Z_{x,y}$ and $U_{x,y}$ denote the components of the vector-functions $\mathbf{Z}$ and $\mathbf{U}^\dagger$.

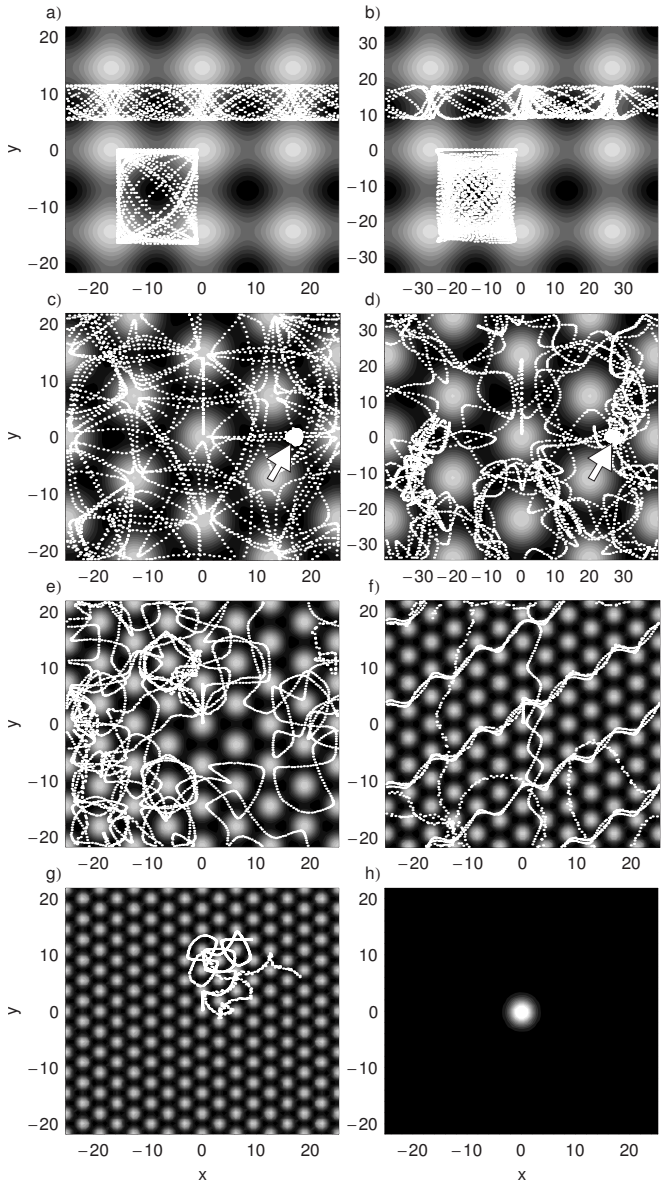

FIG. 2. Chaotic and regular soliton peak trajectories in square (a), (b) and hexagonal (c)–(g) lattices. Dark (light) color indicates higher (lower) values of the refractive index. (a), (c), (e)–(h) correspond to conservative nonlinearity (2). (b) and (d) correspond to dissipative nonlinearity (4) with the same parameter values as in Fig. 1. The modulation amplitude is given by $\varepsilon^2=0.02$ in the conservative case and $\varepsilon^2=0.008$ in the dissipative case. Each of panels (c) and (d) shows two trajectories: one representing a chaotic soliton wandering and the other corresponding to regular oscillations around a minimum of the effective potential. This latter trajectory is indicated by white arrow. (e)–(g) illustrate soliton motion in lattices with different cell size $d_c=4\pi/(3k)$. Here, $k=0.5$ (c), $k=1$ (e), $k=1.5$, (f), $k=2$ (g). The soliton size is approximately visible in (h).

At nonzero ε we will be looking for a slowly moving soliton solution in the form of series expansion $A=\{A_0(|\mathbf{r}'|)+\varepsilon A_1(\mathbf{r}',\varepsilon t)+\varepsilon^2 A_2(\mathbf{r}',\varepsilon t)+\cdots\}e^{i\omega_0 t}$ with $\mathbf{r}'=\mathbf{r}-\mathbf{R}(\varepsilon t)$, where $\mathbf{R}$ is the soliton peak position and $A_{1,2}$ describe small corrections to the soliton shape. Plugging this expansion into Eq. (1) and collecting first-order terms in ε

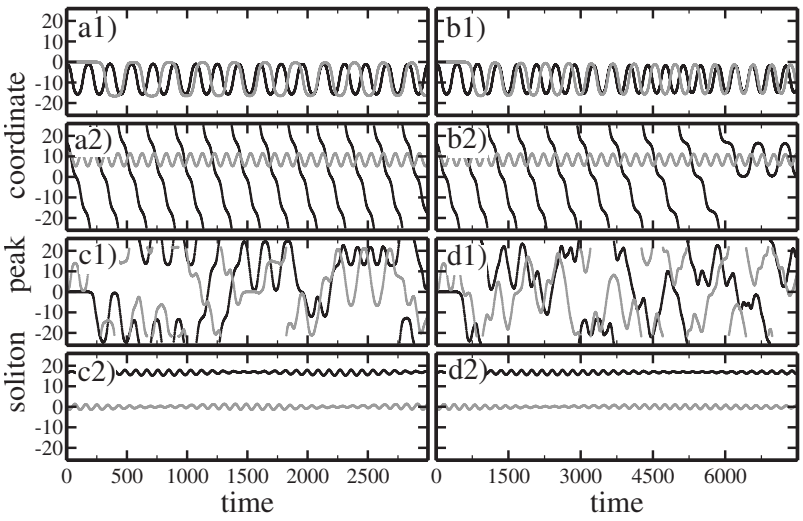

FIG. 3. Time dependencies of the coordinates x (black) and y (gray) corresponding to pairs of the soliton trajectories of Figs. 2(a)–2(d). Panels (a1), (a2), (b1), (b2), (c1), (c2), and (d1), (d2) correspond to the pairs of trajectories shown in Figs. 2(a)–2(d), respectively.

we find that $LA_1=-\dot{\mathbf{R}}\cdot\nabla A_0\equiv-\dot{\mathbf{R}}\cdot\mathbf{U}$ (the dot over $\mathbf{R}$ denotes the derivative with respect to the slow time εt). Since $\mathbf{U}=L\mathbf{Z}$, we may take $A_1=-\dot{\mathbf{R}}\cdot\mathbf{Z}$.

Collecting the second-order terms in ε we obtain $LA_2=-\ddot{\mathbf{R}}\cdot\mathbf{Z}(\mathbf{r}')-ig(\mathbf{r})A_0(|\mathbf{r}'|)-\mathcal{F}(\mathbf{r}')$, with $\mathcal{F}(-\mathbf{r})=\mathcal{F}(\mathbf{r})$. The solvability of this equation with respect to A_2 requires the orthogonality of its right-hand side to the solutions of the homogeneous equation $L^\dagger X=0$. Thus, by multiplying the right-hand side to $U_x^\dagger(\mathbf{r}')$ and $U_y^\dagger(\mathbf{r}')$, and noticing that $\langle\mathcal{F},U_{x,y}^\dagger\rangle=0$, we find that the solvability condition implies $\ddot{\mathbf{R}}\int\Psi(r)dxdy=2\int g(\mathbf{r}+\mathbf{R})\mathrm{Im}[\mathbf{U}^\dagger(\mathbf{r})A_0(r)]dxdy$. Integrating by parts gives finally the following equation for the soliton motion:

$$\ddot{\mathbf{R}}=-\nabla V(\mathbf{R}),\quad V(\mathbf{R})=-2\frac{\int g(\mathbf{r}+\mathbf{R})\Psi(r)dxdy}{\int\Psi(r)dxdy}. \quad (5)$$

Note that in the Hamiltonian case where f is purely imaginary and A_0 is real, we have $L^\dagger(iX)=iLX$, so $\mathbf{U}^\dagger=i\mathbf{U}=i\mathbf{r}A_0'(r)/r$, and $\Psi(r)=-A_0^2(r)/2$. In the non-Hamiltonian case these relations are no longer true, and we do not have an explicit formula for Ψ.

As we see, both in transparent and active-dissipative media, the transverse soliton motion is described, to the leading order, by the Hamiltonian equation (5). Up to the factor of (-2) the potential is obtained by averaging the refractive index g with a weight which depends on the soliton intensity profile. Note that Eqs. (5) are valid for arbitrary ratio of the soliton width to the characteristic period of the refractive index modulation. When this ratio is small, we obtain $V(\mathbf{R})=-2g(\mathbf{R})$. As the ratio grows, the averaging smooths the inhomogeneity of the refractive index. Therefore, when the soliton is sufficiently wide it moves, essentially, like a free particle.

Being a Hamiltonian system with two degrees of freedom, Eq. (5) may exhibit both regular and chaotic dynamical regimes, depending on the shape of the potential and on the initial conditions. In order to examine how the transverse dynamics of the soliton depends on the structure of the refractive index profile, we consider square, $g=-\cos(kx)-\cos(ky)$, and hexagonal, $g=-\Sigma_{0\le l\le 2}\cos[k(x\cos\frac{\pi l}{3}+y\sin\frac{\pi l}{3})]$, lattices. Here $k=\sqrt{2}\pi/d_c$ for the square lattice and $k=4\pi/(3d_c)$ for the hexagonal one, d_c is the radius of the lattice cell. By Eqs. (5), the effective potential that governs the soliton transverse motion is $V(x,y)=-g(x,y)S(k)$, where the response coefficient S is defined by $S(k)=2\frac{\int\cos(kx)\Psi(r)dxdy}{\int\Psi(r)dxdy}$. In the limit of a narrow soliton $(k\to 0)$, we have $S(k)\to 2$, while in the opposite limit $k\to\infty$ the response function decays exponentially. In Fig. 1 we plot the graph of the amplitude profile and the response coefficient for the solitons whose dynamics we studied in our numeric simulations. It is seen that $S(k)$ is not negligibly small, hence the effect of the inhomogeneity of the refractive index profile on the soliton motion is not negligible, for the soliton sizes up to roughly $2d_c$.

In the case of square lattice, the effective potential $V=S(k)[\cos(kx)+\cos(ky)]$ is separable, therefore Eq. (5) is integrable, which means a quasiperiodic motion for the soliton. This is confirmed by direct numerical integration of Eq. (1). Indeed, as we see in Figs. 2(a) and 2(b) the soliton in the square lattice is either trapped in a lattice cell and oscillates quasiperiodically in it, or the quasiperiodic oscillations accompany a constant velocity drift. The picture is the same both for the conservative nonlinearity (2) and for the active-dissipative case (4). However, in the non-Hamiltonian case we may see [Fig. 3(b)] a slow decay in the oscillation amplitude, due to higher order corrections neglected in our derivation of Eq. (5).

The hexagonal refractive index lattice induces a different type of soliton motion, as the hexagonal potential is known to create chaotic dynamics [19]. Namely, while low-energy oscillations near the minimum of the potential remain typically quasiperiodic (by Kolmogorov-Arnold-Moser theorem), the increase of the energy leads to a random walk between the cells. When the energy is close to the maximum of the potential $[V_{max}=3S(k)]$, the motion can be roughly modeled by a bouncing between the points of maximum, with the direction of the velocity changing approximately to 180°, ±150°, ±120°, or ±90° at each bounce; the chaotic

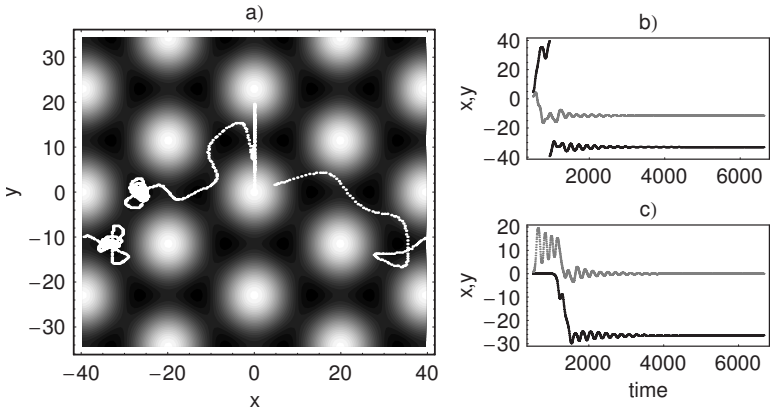

FIG. 4. Soliton motion in an active-dissipative medium with nonzero spatial spectral filtering coefficient $\delta=0.01$. Parameters of nonlinear function (4) are the same as in Figs. 1, 2(d), and 3(d1). (a) A pair of soliton trajectories. (b), (c) The corresponding time dependencies of the coordinates x (black) and y (gray).

character of the motion manifests itself in that the choice between these possibilities is random. The time between the bounces (estimated as a modulation period over $\sqrt{V_{max}}$) defines the scale after which the motion can be considered a random walk. Numerical simulations both for conservative (2) and active-dissipative (4) nonlinearities in Eq. (1) confirm this description, and show either low-amplitude regular oscillations or chaotic wanderings of the soliton peak, see Figs. 2(c), 2(d), 3(c), and 3(d).

The effect of the decrease of the lattice cell size on the soliton motion is illustrated in Figs. 2(e)–2(g). For soliton radii up to $\sim 1.5d_c$ we see a behavior resembling that of a particle in the potential. This is either the random walk described above, or the so-called Levi flights [19] which appear on the boundary between hyperbolic (chaotic) and elliptic (quasiperiodic) behavior in the phase space [see Fig. 2(f)]. In Fig. 4 we present the results of numerical integration of Eqs. (1) and (4) with the "diffusion" term $\delta\Delta A$ added into the right-hand side (for a derivation of this term in a broad area laser model see Ref. [20]). Real and small $\delta>0$ correspond to a spatial spectral filtering, which breaks the Galilean symmetry of Eq. (1) at $\varepsilon=0$. One can show that taking it into account results in adding the dissipation term $\gamma\dot{\mathbf{R}}$ in the left-hand side of Eq. (5), with $\gamma=O(\delta/\varepsilon)$. Indeed, we see in Fig. 4 a steady decrease of the amplitude of oscillations, regular and chaotic alike. In this case the soliton transverse motion finally halts at some position corresponding to a local maximum of the refractive index. The data obtained by direct simulation of Eq. (1) (see Figs. 2–4) are in agreement with the results of numerical solution of the reduced equation (5).

To conclude: we have established a chaotic character of motion of a soliton in hexagonal lattice, even for a weak amplitude of the spatial modulation. Effectively, the soliton performs a random walk characterized by the long-term conservation of the soliton motion energy. This effect takes place both in the case of conservative and dissipative nonlinearity and has a universal nature solely attributed to the Galilean symmetry of the unperturbed system. Factors that destroy this symmetry, e.g., spatial spectral filtering, impede the soliton motion and lead to a halt of the random walk.

This work was supported by Grants No. ISF 273/07, MNTI-RFBR No. 06-01-72023, DFG Research Center MATHEON, Grant No. SFB787 of the DFG, and Center for Advanced Mathematical Studies in Ben Gurion University.

[1] Y. Kivshar and G. Agrawal, *Optical Solitons: From a Fiber to Photonic Crystals* (Academic Press, New York, 2003).
[2] R. Y. Chiao, E. Garmire, and C. H. Townes, Phys. Rev. Lett. **13**, 479 (1964).
[3] M. Vakhitov and A. Kolokolov, Radiophys. Quantum Electron. **16**, 783 (1975).
[4] K. Staliunas, R. Herrero, and G. J. de Valcarcel, Phys. Rev. A **75**, 011604(R) (2007).
[5] *Photonic Crystals: Advances in Design, Fabrication, and Characterization*, edited by K. Busch, R. B. Wehrspohn, S. Lölkes, and H. Föll (Wiley-VCH, New York, 2004).
[6] F. Abdullaev, *Theory of Solitons in Inhomogeneous Media* (Wiley, New York, 1994).
[7] *Nonlinear Photonic Crystals*, edited by R. E. Slusher and B. J. Eggleton, Springer Series in Photonics Vol. 10 (Springer, Berlin, 2003).
[8] Y. Sivan, G. Fibich, and M. I. Weinstein, Phys. Rev. Lett. **97**, 193902 (2006); Physica D **217**, 31 (2006).
[9] A. G. Vladimirov, D. V. Skryabin, G. Kozyreff, P. Mandel, and M. Tlidi, Opt. Express **14**, 1 (2006).
[10] K. Gorshkov and L. Ostrovsky, Physica D **3**, 428 (1981).
[11] Y. S. Kivshar and B. A. Malomed, Rev. Mod. Phys. **61**, 763 (1989).
[12] N. N. Akhmediev, A. Ankiewicz, and J. M. Soto-Crespo, Phys. Rev. Lett. **79**, 4047 (1997).
[13] V. V. Afanasjev, B. A. Malomed, and P. L. Chu, Phys. Rev. E **56**, 6020 (1997).
[14] A. G. Vladimirov, G. V. Khodova, and N. N. Rosanov, Phys. Rev. E **63**, 056607 (2001); A. G. Vladimirov, J. M. McSloy, D. V. Skryabin, and W. J. Firth, *ibid.* **65**, 046606 (2002); D. Turaev, A. G. Vladimirov, and S. Zelik, *ibid.* **75**, 045601(R) (2007).
[15] R. Scharf and A. R. Bishop, Phys. Rev. E **47**, 1375 (1993).
[16] S. Longhi, Phys. Rev. E **55**, 1060 (1997).
[17] Y. V. Kartashov, L. Torner, and V. A. Vysloukh, Opt. Lett. **29**, 1102 (2004).
[18] N. Rosanov, *Transverse Patterns in Wide-Aperture Non-Linear Optical Systems* (North-Holland, Amsterdam, 1996), Vol. XXXV.
[19] G. M. Zaslavsky, R. Z. Sagdeev, and A. A. Chernikov, Sov. Phys. JETP **67**, 270 (1988).
[20] K. Staliunas, Phys. Rev. A **48**, 1573 (1993).